Appl. Phys. B 48, 155–164 (1989)

Applied Physics B Photophysics and Laser Chemistry

Application of a Pulsed Laser for Soot Measurements in Premixed Flames

P.-E. Bengtsson and M. Aldén

Combustion Centre, Lund Institute of Technology, P.O. Box 118, S-22100 Lund, Sweden

Received 19 July 1988/Accepted 11 September 1988

Abstract. A pulsed Nd:YAG laser has been used to perform scattering/extinction measurements in flat, premixed methane/oxygen flames to determine soot particle sizes, number concentrations and soot volume fractions. A discussion is given on accuracies in these determinations with respect to experimental and theoretical parameters. Absorptions were measured through a referencing method which yielded a single-pulse relative standard deviation in the normalized signal of 0.7%. The incident laser fluence was kept below 0.1 J/cm^2 in the focusing point in the flame to avoid soot vaporization effects. Interference in the measurements from polyaromatic hydrocarbons (PAH) is also discussed.

PACS: 78.35, 82.40

The current environmental situation with large amounts of air pollutants caused by inefficient combustion has led to an intensification of research in the field of combustion. Apart from the harmful production of nitric and sulphur oxides, much interest has been focused on the soot formation problem and different aspects have been reviewed in [1–6]. To obtain a basic understanding of the causes of soot emission from, e.g., Diesel engines and coal-fired power plants, there is a need for fundamental studies in well-defined combustion systems. There are several reasons for using premixed, laminar flames for fundamental soot research, for example, the possibility of producing a one-dimensional flame and the easier characterization of parameters such as the C/O ratio (the ratio between the contents of carbon and oxygen atoms in the fuel-oxidant mixture), which have no obvious meaning for a diffusion flame. Diffusion flames can be more difficult to investigate due to, for example, curved streamlines but are interesting to study since they more often resemble real combustion situations. Since the subject in this work was premixed flames the following discussion will be concentrated on this phenomenon.

To characterize a flame, it is important to accurately measure species concentrations and temperatures. This can be achieved non-intrusively using optical techniques, often powerful laser techniques, as long as the incident fluence (pulse energy/unit area) is low enough not to cause optical breakdown or photodissociation of molecules or vaporization of particles. Also, high spatial resolution can be achieved by focusing the laser beams with lenses. Laser techniques widely used for diagnostics of combustion processes are Coherent Anti-Stokes Raman Scattering (CARS) [7–9], Raman Scattering [9, 10] and Laser-Induced Fluorescence (LIF) [9, 11]. CARS can be used for measurements of temperature and major species concentrations (>1%). Raman Scattering is used for both temperature and concentration measurements, but since the signal is very weak it is difficult to use the technique in a hydrocarbon-fuelled combustion process, which itself has a strong emission and where laser-induced fluorescence from large molecules and particles may mask the weak Raman signals. In this case the CARS technique is superior. For measurements of minor species, laser-induced fluorescence is preferable. Besides species concentrations and temperatures, a sooty flame is also characterized by the sizes and concentrations of soot particles, which must be determined to obtain a more complete picture of the combustion processes. Along with the build-up of soot, large molecules such as polyaromatic hydrocarbons are formed [12, 13], which are also incorporated into the soot. Once the soot particles are formed, their

growth is relatively well understood [14–17], while there are still various theories for the intermediate steps preceding the initial formation of the soot particles [4] such as polymerization of aromatics, condensation of gas species which then graphitize and nucleation on ions. More intense research concerning the early phases of soot formation processes is therefore justified.

Pulsed laser sources have received increasing attention in combustion research as they allow time-resolved measurements of combustion parameters. In this paper we report on experiments where a pulsed Nd:YAG laser was used for soot particle size, number concentration and soot volume fraction determinations in laminar, premixed, methane/oxygen flames at atmospheric pressure. Soot particle sizes and number concentrations have previously been determined with a combination of extinction measurements with a tungsten strip filament lamp, and Rayleigh scattering measurements using a continuous wave (cw) laser beam directed through premixed, sooty flames [12, 13, 18]. A thorough treatment of sources of errors and accuracies for the technique will be given and a comparison with the cw laser/lamp technique will be made. Pulsed lasers have previously been used for scattering/extinction measurements in sooty diffusion flames [19], however, the potential of the technique was not discussed. Another technique, which has been used for soot particle measurements is Dynamic Light Scattering (DLS) [20–22], which is based on the broadening of a spectral line which has been scattered from molecules or particles undergoing Brownian motion.

Evaluation of soot particle properties from scattering/extinction measurements is based on the Rayleigh theory for isotropic spheres assuming diameters much less than the used laser wavelength, approximately $d/\lambda \lesssim 0.1$. Also assuming an aerosol with a monodisperse size distribution, the scatter factor, Q_{VV} (the first index denotes the polarization of the scattered light and the second index the polarization of the incident light, V: vertical) is given by [23]

$$Q_{VV} = \frac{1}{4} \cdot \left(\frac{\pi}{\lambda}\right)^4 \cdot F(\tilde{m}) \cdot N \cdot d^6, \qquad F(\tilde{m}) = \left|\frac{\tilde{m}^2 - 1}{\tilde{m}^2 + 2}\right|^2, \quad (1)$$

where $\tilde{m} = n - ik$ is the complex refractive index of the particle, d is the particle diameter, λ is the wavelength of the incident laser light and N is the particle number concentration [cm^{-3}].

The extinction coefficient K_{ext} is given by [23]

$$K_{ext} = \frac{\pi^2}{\lambda} \cdot E(\tilde{m}) \cdot N \cdot d^3, \qquad E(\tilde{m}) = -\mathrm{Im}\left\{\frac{\tilde{m}^2 - 1}{\tilde{m}^2 + 2}\right\} \quad (2)$$

in the Rayleigh regime, and is approximately equal to the absorption coefficient, which means that extinction due to scattering is negligible. By combining (1 and 2), the number concentration and size can be evaluated through the experimentally determined scatter factor Q_{VV} and extinction coefficient, K_{ext}. Inherent theoretical parameters, such as the shape and width of the soot particle size distribution and the complex refractive index of soot, must then be assigned values from literature, unless experimentally determined, and uncertainties in these values can lead to a considerable inaccuracy in the evaluated soot parameters.

In the next section the experimental set-up is described followed by sections describing the measurements. The paper is concluded with a discussion of the results and a summary.

1. Experimental Set-Up

The experimental set-up for the scattering/extinction measurements is shown in Fig. 1. Three sooty, pre-

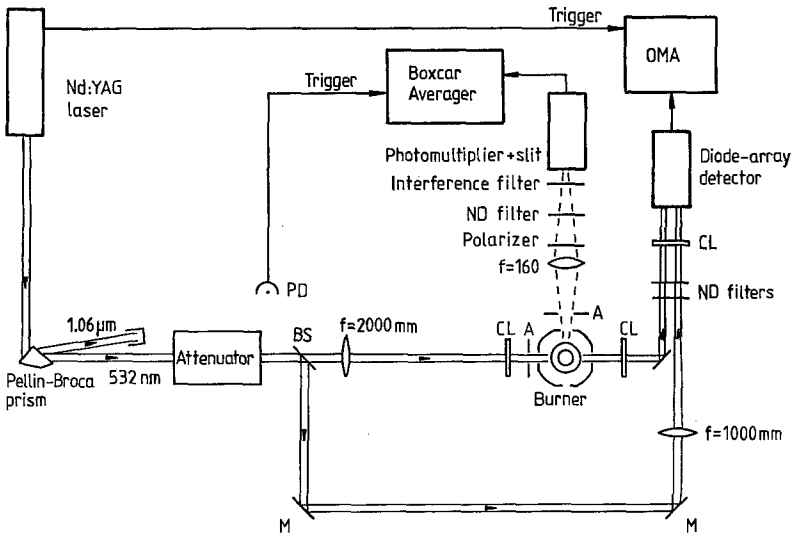

Fig. 1. Experimental Set-up. BS: Beam Splitter, M: Mirror, CL: Cylindrical Lens, PD: Photodiode, and A: Aperture

mixed, methane/oxygen flames with C/O ratios of 0.50, 0.54, and 0.62 were investigated under atmospheric pressure conditions. A water-cooled porous-plug burner produced an approximately one-dimensional flame in the region where the measurements were performed, up to 10 mm above the burner. A flame-stabilizing steel plate was placed 30 mm above the burner platform. The diameter of the burner was 40 mm and the volume flow was constant (5.4 l/min at STP) for all flames. The sooty region of the methane/oxygen flames under study started around 3 mm above the burner. This separation was of great importance, since no unwanted scattering contribution from the burner was observed when the laser was focused 3 mm above the burner surface. Imaged scattering measurements were performed to test the flat flame approximation, as described in the next section. To probe at different heights in the flame, the burner was moved vertically by micro-adjustments.

The light source used for the scattering and extinction measurements was a pulsed Nd:YAG laser (Quanta Ray DCR-1) with a pulse duration of ~ 8 ns. The Infra-Red (IR) beam at 1064 nm was frequency doubled to green light at 532 nm and residual IR radiation was separated from the green light with a Pellin-Broca prism. For the extinction measurements the pulsed laser beam was split into two components, one traversing the flame and one acting as a reference. The beams were directed to spatially separated parts of a diode-array detector and the signals were processed by an optical multichannel analyser (OMA III, EG&G PARC), consisting of 1024 diode elements, each 2.5 mm $\times$ 25 μm. After splitting, the laser beams each had a pulse energy of 0.5 mJ and on the way to the diode-array detector, they had to be attenuated by about 8 orders of magnitude to avoid saturation of the diode array elements. The beams originally had a diameter of 8 mm, but were slightly converged by lenses with long focal lengths so that when reaching the diode array, the beams covered approximately 150 pixels ≈ 3.5 mm. As the diode array has a height of only 2.5 mm, a cylindrical lens was used to focus the beams vertically in order to collect all the light. When the diode-array was placed in the focal plane of the cylindrical lens, strong saturation of the diode-array elements was observed, an effect which was avoided by slight defocusing.

A photomultiplier (EMI 9558 QB) and a BOXCAR integrator (EG&G, PARC) were used for the detection of the scattered light. The laser pulse entering the flame was vertically focused with a cylindrical lens ($f = 350$ mm). The pulse energy was attenuated to 0.5 mJ to avoid soot vaporization effects, which will be discussed in the next section. The beam waist at focus was determined by vertically translating a razor-blade through the beam and registering the signal on the diode-array detector. Ninety percent of the laser light was found to pass within 150 μm. The width of the laser sheet in the flame was 5 mm and the polarization of the beam, when traversing the flame, was better than 200:1. The scattered light was collected perpendicularly to the laser beam, with an $f = 160$ mm lens and imaged (1 : 1) on the detector slit, which had a height of 1 mm and a width of 5 mm. A narrow-band interference filter, $\delta\lambda = 3$ nm, suppressed wavelengths other than the scattered one at 532 nm. A polarizer with an extinction ratio of 10^{-4} was set to transmit light of either horizontal or vertical polarization. Since the scattering intensity varied over 5 orders of magnitude in the measurements, neutral density filters were used to ensure a linear response of the photomultiplier. A detector gate of 100 ns was used, and the trigger pulse was taken from the laser light via a photodiode. Throughout the experiments spurious light, such as reflections from glass surfaces, laboratory walls etc., was minimized by the use of apertures and metal surfaces painted dull black.

2. Preparatory Measurements

Prior to the measurements of scattering and extinction profiles in the sooty flames, preliminary investigations, such as checking the validity of the assumption of a one-dimensional flame were performed. Therefore, the laser light was directed through the flame and focused with an $f = 500$ mm lens and, to avoid laser vaporization of the soot particles, the pulse energy was restricted to 5 μJ. The laser light traversing the flame was imaged, with a magnification ratio of ~ 0.2, onto a diode-array detector with an $f = 40$ mm camera lens. Figure 2 shows a single-shot image from a sooty flame, with an almost uniform scattering pattern. Detector gating and a narrow-band interference filter

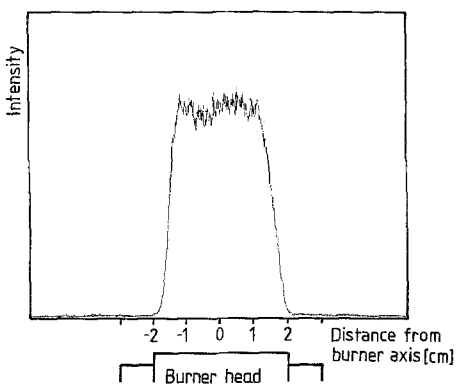

Fig. 2. Single-pulse scattering image from a sooty flame, used to confirm the validity of the assumption of a one-dimensional flame

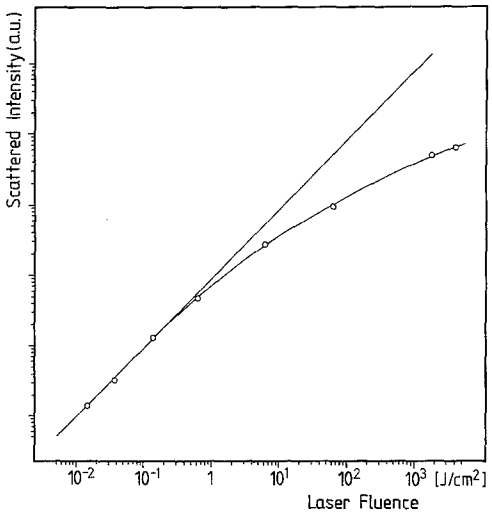

Fig. 3. Scattered intensity as a function of laser fluence, which does not show a linear relationship for fluences above 0.1 J/cm^2 due to vaporization of soot particles

($\delta\lambda = 3$ nm) were used to suppress the flame emission to a negligible level compared with the scattering.

Another effect which has to be confirmed is the linear dependence of the scattering signal on the incident laser fluence, which means that no significant vaporization of the soot particles occurs in the region under study. Laser vaporization of soot has previously been observed for laser fluences of a few J/cm^2 in sooty flames [24, 25]. The dependence of the scattering signal intensity on the incident laser fluence was studied by focusing the laser beam in the flame with an $f = 500$ mm lens and recording the scattered light perpendicular to the laser beam using a photomultiplier. As can be seen in Fig. 3, the detected scattering signal deviated from the linear relationship with the incident fluence when the laser fluence exceeded ~ 0.1 J/cm^2. Even if the higher fluences totally vaporize the soot particles in the laser beam centre, scattering signals will be registered which have their origin in the wings of the laser beam profile. Thus, when scattering/extinction measurements are performed, the incident fluence must be below 0.1 J/cm^2 in order not to significantly vaporize the soot particles. For very high laser fluences ($> 10^2$ J/cm^2 for this set-up), laser-induced C_2 emission from the Swan bands can be observed, an effect which is not completely understood. This feature and the correlation to soot profiles are currently under investigation [26].

3. Scattering/Extinction Measurements

For the extinction measurements the ratio between the intensities of the signal and the reference beam was registered as described in Sect. 1. However, in a first approach, each beam was directed to separate photodiodes connected to a BOXCAR integrator on which the signals were recorded and consequently divided. With this arrangement, the single-shot relative standard deviation of the normalized signal intensity was around 4%. Since lower pulse-to-pulse fluctuations in the normalized signal were desired, the method mentioned above where the two beams were directed to spatially separated parts of a diode-array detector was investigated. With this method the relative standard deviation of the registered laser pulse intensity using single pulses was around 2.0%, but could be reduced to $\sim 0.7\%$ by normalization with a reference beam. In these measurements 20 single shots were averaged, which reduced the relative standard deviation to $\sim 0.15\%$, for the normalized signal. An absorption was thus detected as a displacement from the normalized signal level and the detection limit was of the order of 0.2%. In these flame measurements no absorption less than 1% was considered. The flames were investigated up to a height of 10 mm above the burner, since at this height the Rayleigh equations could still be used. The extinction coefficient is then equal to the absorption coefficient, which was experimentally determined as

$$K_{\text{ext}}(\approx K_{\text{abs}}) = \frac{1}{L}\ln(E_O/E_T), \tag{3}$$

where L is the transmission length in the sooty flame in cm, E_O is the incident laser pulse energy and E_T is the transmitted laser pulse energy. The flame length at each height was determined from photographs, which is the conventional approach. Flame length determination can, when the scattering is strong enough, also be made from imaged scattering measurements.

In the scattering measurements, the scatter factor can be determined from measurements of scattering volumes, solid angles and laser intensities, as performed by d'Alessio et al. [12]. A simpler approach, later used by d'Alessio et al. [18], was applied in these studies, where the scattering signal from the sooty flame was internally calibrated by the scattering signal from flowing gases with well-known cross-sections. In these experiments methane and nitrogen were used as calibration gases, and were passed through the burner at room temperature and atmospheric pressure. The scatter factor from a gas can be expressed as [27]

$$Q_{\text{VV}} = \frac{4\pi^2}{\lambda^4}\cdot\frac{(n-1)^2}{N}\cdot\left(\frac{3}{3-4\varrho_V}\right), \tag{4}$$

where the number concentration N can be calculated from the ideal gas law and values of the refractive index n, and the depolarization ratio, ϱ_V, can be found in the literature [27, 28].

The results from the scattering measurements are shown in Fig. 4. A steep rise – around 5 orders of

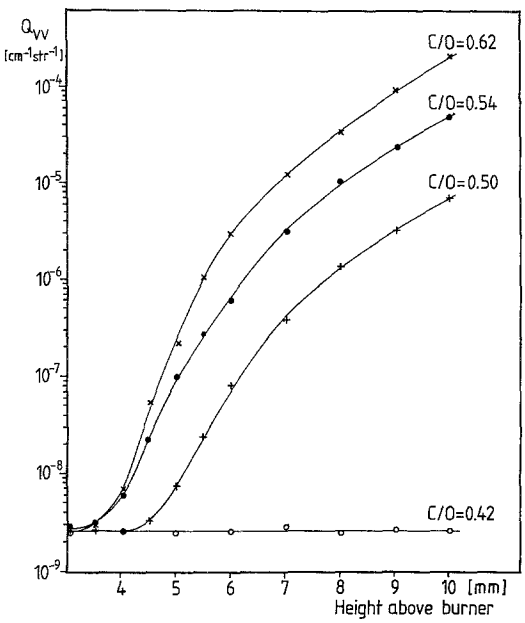

Fig. 4. The scatter factor Q_{VV}, versus height above the burner for sooty methane/oxygen flames at different C/O ratios and a non-sooty flame with C/O = 0.42

magnitude – can be observed in the scattering signal from the sooty flames up to 10 mm above the burner. The scattering from the flame gases in a non-sooty flame with C/O = 0.42 was measured and subtracted from the scattering signals from the sooty flames to obtain correct evaluations of soot particle sizes and concentrations, especially in the lower regions of the flames. The scattered signal was also compensated for absorption by the soot – with values from the extinction measurements – since the incident light was attenuated before scattering occurred and the scattered light was attenuated by soot on its way to the detector. The flame emission contribution to the scattered signal was reduced by detector gating and an interference filter so that the contribution to the vertically scattered component for all flame points was less than 1%. The detection limit for this experimental set-up was $Q_{VV} \approx 3 \times 10^{-11}$ cm^{-1} str^{-1}.

The depolarized scattered component from spherical Rayleigh scatterers is assumed to be zero, however, experimentally a depolarized "scattering" signal was detected which strongly increased as a function of height above the burner. There are two main contributions to this depolarized component, Q_{HV}. One is unpolarized fluorescence from polyaromatic hydrocarbons (PAH), which increases slowly with increasing height above the burner (see next section) but will give the strongest interference in the lower part of the sooty region. The other is a depolarized component of the elastically scattered light which has its origin in anisotropy in particle shape and polarizability [13]. The depolarization ratio, $\varrho_V = Q_{HV}/Q_{VV}$, did reach values up to 50% around 4 mm above the burner and at heights above 6 mm above the burner had values below 2%. Thus, it is especially important to subtract the depolarized component from the polarized component in the lower regions of the sooty flames in order to evaluate correct particle sizes and number concentrations.

4. Laser-Induced Fluorescence Measurements

The unpolarized fluorescence observed in the sooty regions of premixed flames is attributed to polyaromatic hydrocarbons (PAH) [12, 29, 30]. PAH constitute a group of molecules which mainly consist of a small number of benzene rings, often 2–5, and support has been given for their role in soot formation processes as intermediate species [31]. Sampling methods with chromatographic and/or mass spectrometric detection of PAH have been used to separate them [12, 32], but have the disadvantage of perturbing the flame processes. Optical methods have the feature of being non-intrusive but the broadband unstructured fluorescence from the polyaromatics [33–35] makes it difficult to separate them.

The spectral shape of the PAH fluorescence was measured for the three investigated sooty flames in the region 4–10 mm above the burner. Figure 5 depicts the spectral distribution of the depolarized light at a height of 5 mm above the burner in the methane/oxygen flame with C/O = 0.62. Superimposed on the broadband fluorescence structure between 400 and 750 nm, the depolarized elastically scattered component at 532 nm can be observed. The broadband fluorescence from the methane/oxygen flames peaked around 540 nm, and as it was found that the spectral shape of the fluorescence was approximately the same for the three sooty flames at all heights in the present study, only a portion of the spectra, which were unaffected by the depolarized component at 532 nm, was treated when comparing

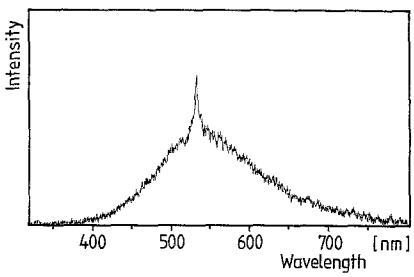

Fig. 5. Spectral distribution of unpolarized polyaromatic hydrocarbon fluorescence for a methane/oxygen flame with C/O = 0.62, 5 mm above the burner. The peak at 532 nm is the depolarized component scattered by the soot. The spectrum is the result of 100 single-shots

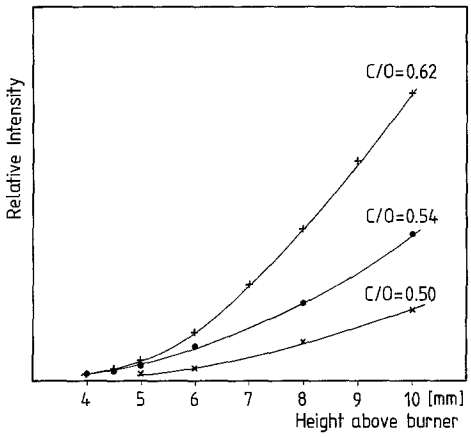

Fig. 6. PAH-fluorescence signal profiles for the investigated methane/oxygen flames

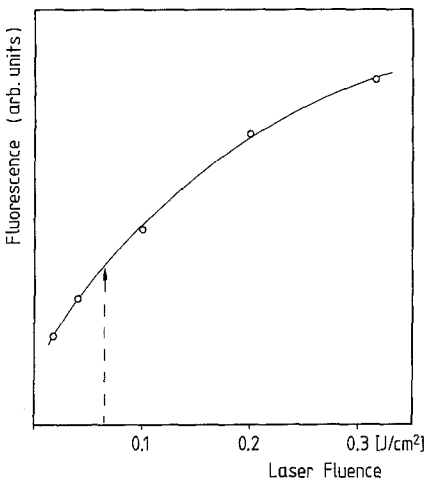

Fig. 7. Fluorescence signal from polyaromatic hydrocarbons versus laser fluence for a flame with C/O = 0.62, 5.5 mm above the burner. The arrow indicates the laser fluence used in the scattering measurements

the fluorescence signals as represented in Fig. 6. The fluorescence signal thus increases as a function of height above burner and as a function of C/O ratio. Even if the PAH fluoresce more at greater heights, their greatest interference with the scattering is in the soot inception zone where the fluorescence and the scattering are of the same magnitude.

Another feature observed for the PAH fluorescence was saturation of the fluorescence signal when increasing the incident fluence of the pulsed laser beam, as illustrated in Fig. 7, where the arrow indicates the laser fluence used in the scattering measurements. The saturation corresponds to the statement by Smyth et al. [36], that absorption by polyaromatic hydrocarbons consists of one-photon allowed transitions which are easily saturated. This observation of saturation may imply that the ratio between PAH absorption and soot absorption is less for this technique compared with the cw laser/lamp technique. A rough estimate of this ratio can be made by referring to Fig. 5. The ratio between the spectrally integrated fluorescence and depolarized scattering attributed to soot is defined as b, when corrected for spectral variation in the detector quantum efficiency. Let the relation between the scattering efficiency from soot and absorption efficiency by soot be specified by the factor c, the ratio between depolarized and polarized scattering from soot by a factor d and the fluorescence yield in the visible region Φ. Then the ratio between the PAH absorption and soot absorption, e, can be estimated through the formula

$$e = b \cdot \frac{c \cdot d}{\Phi}. \tag{5}$$

For the flame point in Fig. 5, C/O = 0.62 at a height of 5 mm above the burner, $b \approx 50$ and $c \approx 10^{-4}$. An appropriate value of d is ~ 0.02 and $\Phi \approx 10^{-2}$ [13], and together such a low estimated value as $e \approx 10^{-2}$ will be obtained for the ratio between PAH absorption and soot absorption 5 mm above the burner, i.e. 2 mm into the sooty region of the flame.

5. Results and Discussion

Soot particle size and concentration profiles were evaluated from the scattering and extinction equations (1 and 2), and the size profiles are shown in Fig. 8. A monodisperse soot aerosol is then assumed with a soot particle refractive index of $\tilde{m} = 1.9 - 0.55i$ [37]. The increase in the soot particle size with height is very rapid due to surface growth and coagulation processes with the steepest rise for the most sooty

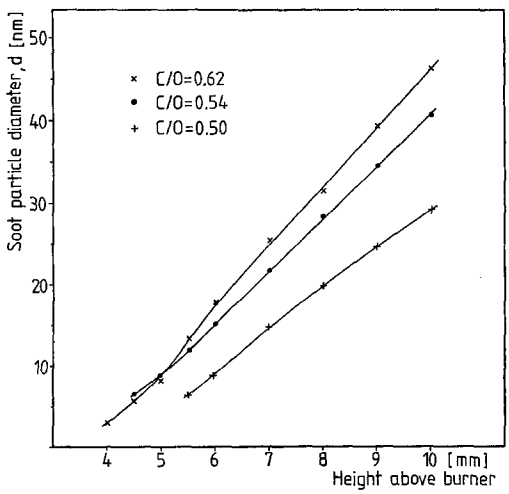

Fig. 8. Soot particle size profiles evaluated from the Rayleigh scattering/extinction equations

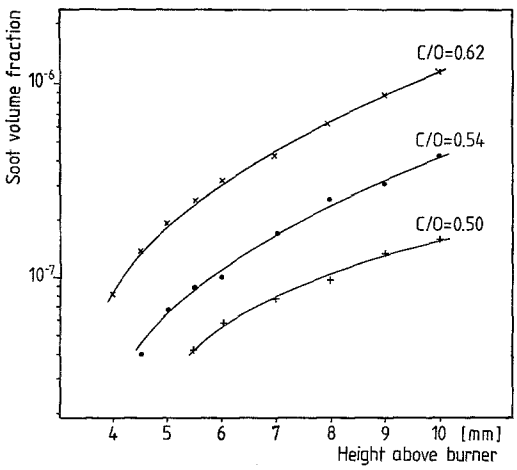

Fig. 9. Soot volume fraction profiles converted from the extinction coefficients

flame. After initial concentrations higher than $10^{11}\,\mathrm{cm}^{-3}$, a fast decrease occurred to concentrations around $10^{10}\,\mathrm{cm}^{-3}$ at 10 mm above the burner. The decrease is due to coagulation, which is the only process affecting the concentrations beyond the soot nucleation zone. In Fig. 9 the soot volume fraction profiles (f_V) are presented, which can be simply calculated from the profiles of N and d through the formula $f_V = \pi \cdot N \cdot d^3/6$. However, the Nd^3 term is directly measured in the extinction coefficient and the soot volume fraction can be deduced through the expression

$$f_V = \frac{1}{6} \cdot \frac{K_{ext} \cdot \lambda}{\pi \cdot E(\tilde{m})}. \tag{6}$$

The curves reveal that only a small part of the total soot volume is due to the soot nucleation process, instead surface growth reactions are predominant.

The accuracy in the evaluated numbers is limited both by experimental and theoretical uncertainties. When considering the experimental uncertainties, the inaccuracy in the extinction measurements will be due to the general problem of accurately measuring small absorptions, part of the absorption may be due to large molecules such as polyaromatic hydrocarbons and some uncertainty in the determination of the flame length. The flame length is generally determined from flame photographs and taken as the luminous flame width, which is assumed to correspond to a uniform absorption path length. The error in the flame length determination can be estimated to be less than 5%.

To estimate the accuracy in the absorption measurements, a study of the signal processing is performed. Each of the beams (signal and reference) covered around 150 diode-array pixels with approximately 5000 counts in each, which led to a total value of $\sim 7 \times 10^5$ counts, which originated from $\sim 7 \times 10^6$ photons [38] leading to a Poisson noise of less than 0.1%. However, in practice the relative standard deviation for the normalized single-shot signal was 0.7% and the main contribution to this may be noise due to differences in the detector characteristics for the different parts of the diode array [39]. When 20 shots were averaged in these measurements, the relative standard deviation for the normalized signal was reduced to 0.15% and for such low values other noise sources such as detector read-out noise will obtain increasing importance. An absorption of 5% can, with this technique in single-shot performance, be estimated to be measured with an accuracy of 20%, which in these measurements was reduced to 4% when 20 shots were averaged in each data point.

Concerning the accuracy in the scattering measurements, a potential uncertainty is the scattering calibration with a methane gas flow. The maximum difference between such calibrations was 5%. The flame emission contribution to the vertically polarized scattering signal was reduced to less than 1% for all flames using detector gating and interference filters. The relative standard deviation of the scattered signal on the photomultiplier was typically around 6% due to flame fluctuations, laser pulse-to-pulse fluctuations and detector noise. Averaging over 20 shots, led to a reduction in this number to ~3%. At the first flame points, where scattering from soot occurs, the accuracy is worse because of the need to subtract both flame gas scattering and depolarized "scattered" light. From the foregoing reasoning, accuracies in the determination of Q_{VV} and K_{ext} can be estimated and these are given in Table 1 for two flame points, 5 and 10 mm above the burner for a flame with C/O = 0.54. The accuracies for single-shot measurements are also calculated for the higher flame point. The dependence of N, d, and f_V on the experimentally obtained parameters are K_{ext}^2/Q_{VV}, $(Q_{VV}/K_{ext})^{1/3}$ and K_{ext}, respectively, and accuracies in these are also presented in Table 1. It can thus be seen that, from an experimental point of view, the most reliable determination is of the soot particle size and the least accurate of the soot particle concentration. An effect which has not been taken into account in Table 1 is the inaccuracy introduced by a low spatial resolution in the flame measurements. From Fig. 8 it can be seen that the soot particle size will increase ~1 nm over a length of 150 μm which was approximately the resolution in the measurements.

When comparing different experimental approaches, the scattering/extinction method using a cw laser for the scattering measurements and a tungsten strip filament lamp for the extinction measurements will of course have the same theoretical limitations as

Table 1. The estimated accuracies in the experimental parameters for three experimental situations. In the last columns it is shown how they contribute to the accuracy (rms values) in the evaluated soot particle properties. x is the height above the burner

Flame condition	Q_{VV}	$K_{ext} \sim f_V$	$K_{ext}^2/Q_{VV} \sim N$	$\left(\frac{Q_{VV}}{K_{ext}}\right)^{1/3} \sim d$
C/O = 0.54 x = 5 mm	8%	15%	23%	6%
C/O = 0.54 x = 10 mm	6%	6%	10%	3%
C/O = 0.54 x = 10 mm single-shot	8%	12%	19%	5%

the pulsed laser technique. Experimentally, the cw laser/lamp technique is limited to stationary phenomena, whereas the short pulse duration of a pulsed laser can be used for the investigation of non-stationary phenomena. With lock-in detection the scattering signal will be "lifted off" the background flame emission for the cw laser/lamp technique, instead of suppressing the background as for the pulsed laser technique. The absorption measurement is more accurate for a lamp than for a pulsed laser even in this approach where the signal is normalized, since the stability of a lamp is of the order of 0.05%–0.1% [13, 18]. However, other referencing methods in absorption measurements with pulsed lasers may be competitive with the lamp technique [40]. Interesting is also the application of this pulsed laser technique in combination with other pulsed laser diagnostic techniques such as CARS.

When discussing the different features of the scattering/extinction techniques, it is appropriate to briefly make some comparisons with the Dynamic Light Scattering technique (DLS) [20–22], which is based on the spectral broadening of light scattered from particles or molecules undergoing Brownian motion. The diffusion coefficient, deduced from the experiment, can be converted to a soot particle size through an experimentally determined temperature and information on parameters such as the fluid viscosity, the mean free path and the nature of particle-molecule collisions. If a monodisperse soot particle size distribution is assumed the soot particle size determination will be independent of the complex refractive index. To obtain the number concentration, Dynamic Light Scattering (DLS) must be combined with a measurement of the static light scattering intensity and then the uncertainty in the complex refractive index will again be introduced. It seems that the dynamic light scattering method does not have the capability to measure as small particles as the scattering/extinction method. The smallest determined particle size for dynamic light scattering in [22] was 70 Å, whereas in these measurements particle sizes down to 30–40 Å were inferred, and for the conventional cw laser/lamp scattering/extinction technique particle sizes down to 15–20 Å [41] have been reported. However, an advantage of DLS compared with the scattering/extinction technique is the possibility of spatially resolved measurements.

Concerning the theoretical limitations, (1 and 2) are based on the assumptions of an optically thin, monodisperse system of spherical scatterers, which have sizes much less than the utilized laser wavelength. Since the evaluated soot particle sizes are less than 1/10 of the laser wavelength 532 nm, the Rayleigh scattering equation is sufficient and no extension to the Mie equations has to be made. When entering the Mie regime, an increased forward scattering can be seen, which can thus be used as an experimental indication that the Rayleigh criterion is becoming invalid. In the Rayleigh regime the scattering is negligible compared with the absorption, and the flame can be regarded as optically thin with a negligible contribution from multiple scattering effects. The assumption of spherical soot particles is acceptable in the early phases of soot formation before chain formation occurs. This has been proven with the aid of electron micrographs which show that the sampled soot particles are spherical [41].

To use the scattering/extinction equations, knowledge of the complex refractive index of soot, $\tilde{m} = n - ik$, is required. The easiest and most general treatment is to select a previously determined value from the literature and apply it at all flame heights. However, the soot particle properties change with flame height, for example, a nucleated soot particle has a high hydrogen content while an aged particle is dehydrogenated [16]. Accordingly, it is not surprising that the complex refractive index of soot changes with height above the burner, as has recently been shown by Charalampopoulos and Felske [22], who performed *in-situ* measurements at different heights in a sooty methane/oxygen flame with a combination of the dynamic light scattering and static light scattering/extinction methods and found an increase in both the real and imaginary parts of the refractive index when the nucleated soot particles are growing. Many techniques have been used to determine the complex refractive index of soot and many of them are questionable, e.g. *ex-situ* measurements which suffer from potential sampling interference [42]. Different complex refractive indices of soot has been suggested, e.g. $\tilde{m} = 1.56 - 0.46i$ [43], $\tilde{m} = 1.9 - 0.35i$ [44], $\tilde{m} = 1.7 - 0.8i$ [45], $\tilde{m} = 2.0 - 1.0i$ [46], and $\tilde{m} = 1.90 - 0.55i$ [37]. When evaluations of d, N, and f_V are made with these

values of $\tilde{m}$, the calculated relative standard deviations in the determination of d, N, and f_V are $\sim 10\%$, $\sim 60\%$, and $\sim 40\%$, respectively.

Another critical assumption is that of a monodisperse size distribution of the soot particles, since several reports have shown that a polydisperse size distribution is a better description of the sooty flame condition. For example, Wersborg et al. [47] found that nucleated soot particles tend to have a narrow Gaussian size distribution, while aged soot particles are better described by a broader logarithmic normal distribution. Support for a logarithmic normal distribution has also been found in other studies [41, 45], where the sampled soot particles were analysed by electron microscopy. Another size distribution, the self-preserving size distribution (SPSD), suggested by Lai et al. [48], is reached during flame conditions where free-molecule coagulation theory from Brownian motion is applicable. As a sooty flame region is covered, which exhibits nucleation as well as coagulation and surface growth, it is difficult to assume correct distributions and correct widths at the different flame heights. Because of these uncertainties, a monodisperse size distribution has been used in these calculations at all heights. Using this treatment the number concentrations will be underestimated, whereas the particle sizes will be overestimated. The choice of either the monodisperse or the self-preserving size distribution will give a difference in the determination of N of approximately a factor 2. Thus the theoretical uncertainties are significant.

6. Summary

A pulsed Nd:YAG laser has been used to perform scattering/extinction measurements in flat, premixed methane/oxygen flames to determine soot particle sizes, number concentrations and soot volume fractions. The accuracies in these values are limited by uncertainties in experimental and theoretical parameters, where the main theoretical uncertainties are the assumptions of a certain soot complex refractive index and a certain soot particle size distribution. This is a conventional approach, even though the inaccuracies in the determination of soot properties resulting from these assumptions were calculated to be larger than those introduced experimentally. However, in this study, effort was concentrated on the examination of the pulsed laser technique and uncertainties in experimental parameters. In this study a monodisperse size distribution has been chosen and a complex refractive index of $\tilde{m} = 1.9 - 0.55\mathrm{i}$ [37].

Experimentally, inaccuracy in the measurement of the extinction coefficient will arise from the flame length determination, the general uncertainty in the measurement of small absorptions and possible non-soot absorption interference by large molecules such as polyaromatic hydrocarbons in the soot nucleation region. Difficulties in measuring small absorptions with a pulsed laser are due to inherent pulse-to-pulse fluctuations. However, by splitting the laser pulse into a signal beam and a reference beam, and forming the ratio between their intensities, the normalized signal will, to a large extent, be independent of pulse-to-pulse fluctuations and the relative standard deviation of the single-shot normalized signal was 0.7%. By averaging over 20 single-shots, the accuracy in the measurement of an absorption of 5% was $\sim 4\%$.

To avoid soot vaporization, the incident laser fluence in the flame centre was kept below 0.1 J/cm^2, but despite this restriction a high sensitivity in the scattering measurements was achieved. The detection limit was $Q_{VV} \approx 3 \times 10^{-11}\,\mathrm{cm}^{-1}\,\mathrm{str}^{-1}$ and the burnt flame gas scattering was easily detected with $Q_{VV} \approx 2.5 \times 10^{-9}\,\mathrm{cm}^{-1}\,\mathrm{str}^{-1}$. A flame emission contribution to the scattering was reduced to below 1% using detector gating and interference filters.

The unpolarized fluorescence from polyaromatic hydrocarbons was observed to increase strongly with the height above the burner and with the C/O ratio. The PAH fluorescence interference is, however, most serious in the lower part of the sooty flames. At about the laser fluence used in the scattering measurements, saturation behaviour was registered in the fluorescence signal.

Single-shot measurements were also performed and due to the short time scales probed, there is a potential for the application to non-stationary phenomena.

Acknowledgements. The authors gratefully acknowledge the general interest of Sune Svanberg. The work was financially supported by the Swedish National Board for Technical Development (STU) and ABB-STAL AB.

References

1. K.H. Homann: Comb. Flame **11**, 265–287 (1967)
2. B.S. Haynes, H.G. Wagner: Prog. Energy Comb. Sci. **7**, 229–273 (1981)
3. H.F. Calcote: Comb. Flame **42**, 215–242 (1981)
4. A.G. Gaydon: *The Spectroscopy of Flames* (Chapman and Hall, London 1974
5. A.G. Gaydon, H.G. Wolfhard: *Flames: Their Structure Radiation and Temperature*, 4th ed. (Chapman and Hall, London 1979)
6. W.L. Flower: In *Remote Sensing* SPIE **644**, 28–39 (1986)
7. R.J. Hall, A.C. Eckbreth: In *Laser Applications*, Vol. 5, ed. by J.F. Ready, R.K. Erf (Academic, New York 1984) pp. 213–309
8. M. Aldén, H. Edner, S. Svanberg: Phys. Scri. **27**, 29–38 (1983)

9. A.C. Eckbreth, P.A. Bonczyk, J.F. Verdieck: Prog. Energy Comb. Sci. **5**, 253–322 (1979)
10. M. Lapp, C.M. Penney: *Advances in Infrared and Raman Spectroscopy*, Vol. 3, ed. by R.J.H. Clark, R.E. Hester (Heyden, London 1977) pp. 204–261
11. D.R. Crosley, G.P. Smith: Opt. Eng. **22**, 545–553 (1983)
12. A. D'Alessio, A. Di Lorenzo, A.F. Sarofim, F. Beretta, S. Masi, C. Venitozzi: Proc. 15th Int'l Symp. on Combustion, Comb. Inst., Pittsburg (1975) pp. 1427–1438
13. B.S. Haynes, H. Jander, H.G. Wagner: Ber. Bunsenges. Phys. Chem. **84**, 858–592 (1980)
14. G. Prado, J. Lahaye, D. Siegla, G. Smith (eds.): *Particulate Carbon: Formation During Combustion* (Plenum, New York 1981) pp. 143–164
15. H. Bockhorn, F. Fetting, G. Wannemacher, H.W. Wenz: Proc. 19th Int'l. Symp. on Combustion, Comb. Inst., Pittsburg, Pa (1982) pp. 1413–1420
16. S.J. Harris, A.M. Weiner: Comb. Sci. Tech. **31**, 155–167 (1983)
17. S.J. Harris, A.M. Weiner: Comb. Sci. Tech. **32**, 267–275 (1983)
18. A. D'Alessio, A. Di Lorenzo, A. Borghese, F. Beretta, S. Masi: Proc. 16th Int'l Symp. on Combustion, Comb. Inst., Pittsburgh, Pa (1977) pp. 695–708
19. A. Gomez, I. Glassman: Proc. 21 Int'l Symp. on Combustion, Comb. Inst., Pittsburgh, Pa (1986) pp. 1087–1095
20. S.S. Penner, J.M. Bernard, T. Jerskey: Acta Astronautica **3**, 69–105 (1976)
21. W.L. Flower: Comb. Sci. Tech. **33**, 17–33 (1983)
22. T.T. Charalampopoulos. J.D. Felske: Comb. Flame **68**, 283–294 (1987)
23. M. Kerker: *The Scattering of Light and Other Electromagnetic Radiation* (Academic, New York 1969)
24. C.J. Dasch: Opt. Lett. **9**, 214–216 (1984)
25. C.J. Dasch: Proc. 20th Int'l Symp. on Combustion, Comb. Inst., Pittsburg, Pa (1984) pp. 1231–1237
26. P.-E. Bengtsson, M. Aldén: To be published
27. R.R. Rudder, D.R. Bach: J. Opt. Soc. Am. **58**, 1260–1266 (1968)
28. Landolt-Börnstein (Ed.): *Zahlenwerte und Funktionen aus Physik, Chemie, Astronomie, Geophysic und Technik*, II, Band, 8 Teil, Optische Konstanten (Springer, Berlin, Heidelberg 1962)
29. A. Di Lorenzo, A. D'Alessio, V. Cincotti, S. Masi, P. Menna, C. Venitozzi: Proc. 18th Int'l Symp. on Combustion, Comb. Inst., Pittsburg, Pa (1981) pp. 485–491
30. M. Frenklach, J. Warnatz: Comb. Sci. Tech. **51**, 265–283 (1987)
31. J.-L. Delfau, C. Vovelle: Comb. Sci. Tech. **41**, 1–15 (1984)
32. B.D. Crittenden, R. Long: Comb. Flame **20**, 359–368 (1973)
33. J.H. Miller, W.G. Mallard, K.C. Smyth: Comb. Flame **47**, 205–214 (1982)
34. D.S. Coe, B.S. Haynes, J.I. Steinfeld: Comb. Flame **43**, 211–214 (1981)
35. D.S. Coe, J.I. Steinfeld: Chem. Phys. Lett. **76**, 485–489 (1980)
36. K.C. Smyth, J.H. Miller, R.C. Dorfman, W.G. Mallard, R.J. Santoro: Comb. Flame **62**, 157–181 (1985)
37. S.C. Lee, C.L. Tien: Proc. 18th Int'l Symp. on Combustion, Comb. Instr., Pittsburg, Pa (1981) pp. 1159–1166
38. OMA III manual, EG & G PARC
39. R.R. Antcliff, M.E. Hillard, O. Jarrett Jr.: Appl. Opt. **23**, 2369–2373 (1984)
40. U. Wolf, E. Tiemann: Appl. Phys. B **39**, 35–42 (1986)
41. H. Bockhorn, F. Fetting, A. Heddrich: Proc. 21 Int'l Symp. on Combustion, Comb. Inst., Pittsburg, Pa (1986) pp. 1001–1012
42. J.D. Felske, T.T. Charalampopoulos, H.S. Hura: Comb. Sci. Tech. **37**, 263–284 (1984)
43. W.H. Dalzell, A.F. Sarofim: J. Heat Transfer **91**, 100–104 (1969)
44. S. Chippett, W.A. Gray: Comb. Flame **31**, 149–159 (1978)
45. A.B. Pluchino, S.S. Goldberg, J.M. Dowling, C.M. Randall: Appl. Opt. **19**, 3370–3372 (1980)
46. J. Janzen: J. Coll. Interf. Sci. **69**, 436–447 (1979)
47. B.L. Wersborg, J.B. Howard, G.C. Williams: Proc. 14th Int'l Symp. on Combustion, Comb. Inst. Pittsburg, Pa (1973) pp. 929–940
48. F.S. Lai, S.K. Friedlander, J. Pich, G.M. Hidy: J. Coll. Interf. Sci. **39**, 395–405 (1972)